Entropy of single-file water in (6,6) carbon nanotubes

Aparna Waghe,[1,a)] Jayendran C. Rasaiah,[1,b)] and Gerhard Hummer[2,b)]
[1]*Department of Chemistry, University of Maine, Orono, Maine 04469-5706, USA*
[2]*Laboratory of Chemical Physics, National Institute of Diabetes and Digestive and Kidney Diseases, National Institutes of Health, Bethesda, Maryland 20892-0520, USA*

(Received 1 March 2012; accepted 26 June 2012; published online 30 July 2012)

We used molecular dynamics simulations to investigate the thermodynamics of filling of a (6,6) open carbon nanotube (diameter $D = 0.806$ nm) solvated in TIP3P water over a temperature range from 280 K to 320 K at atmospheric pressure. In simulations of tubes with slightly weakened carbon-water attractive interactions, we observed multiple filling and emptying events. From the water occupancy statistics, we directly obtained the free energy of filling, and from its temperature dependence the entropy of filling. We found a negative entropy of about $-1.3\ k_B$ per molecule for filling the nanotube with a hydrogen-bonded single-file chain of water molecules. The entropy of filling is nearly independent of the strength of the attractive carbon-water interactions over the range studied. In contrast, the energy of transfer depends strongly on the carbon-water attraction strength. These results are in good agreement with entropies of about $-0.5\ k_B$ per water molecule obtained from grand-canonical Monte Carlo calculations of water in quasi-infinite tubes in vacuum under periodic boundary conditions. Overall, for realistic carbon-water interactions we expect that at ambient conditions filling of a (6,6) carbon nanotube open to a water reservoir is driven by a favorable decrease in energy, and opposed by a small loss of water entropy. © *2012 American Institute of Physics*. [http://dx.doi.org/10.1063/1.4737842]

I. INTRODUCTION

Water in the interior of narrow carbon nanotubes has unusual structural and thermodynamic properties. Despite their apparent nonpolar character, carbon nanotubes tend to fill with water at ambient conditions, as shown by simulations[1–9] and observed in a broad range of experiments.[10–15] In narrow tubes with subnanometer diameters, water forms a single-file arrangement, in which each water molecule donates one hydrogen bond, and accepts one from another water molecule. Water filling is strongly cooperative and sensitive to small perturbations in interactions with the confining walls[2] and to changes in solvent conditions.[16,17] Water flow rates that far exceed the hydrodynamic predictions of Hagen-Poiseuille flow have been reported,[1,13,14] reflecting the strong coupling between nanoscopically confined water molecules within the tube, and the weaker interactions with the walls. This remarkable transport property and the unexpected thermodynamic stability of the peculiar quasi-1D water structure at room temperature with its high translational order have been examined with molecular simulations and theoretical models.[16,18] Identifying the thermodynamic driving force for water filling is not only of fundamental interest, but is also relevant in the design of nanotube devices, including filters for water purification and solvent separation, in probing the mechanism of water transport in biological channels, and in explaining why "nonpolar" cavities in proteins can occasionally contain water.[17,19]

Despite extensive studies, there are conflicting views of whether filling is driven by the entropy or energy of transfer.[3,16,20,21] The magnitude and even the sign of the entropy of single-file water remain contentious. An early study by Vaitheeswaran *et al.*[3] reported a near-zero entropy of transfer from bulk into a quasi-infinite nanotube obtained by periodic replication of a finite nanotube segment. In these calculations, the thermodynamics of water filling was determined by an explicit calculation of the grand-canonical partition function for the confined water, using the TIP3P model for water in the nanotube and experimental data for the temperature dependence of the chemical potential and density of bulk water. In more recent studies, density of states formalisms were used to estimate the translational and rotational contributions to the entropy, producing positive transfer entropies for model TIP3P and SPC/E water in (6,6) carbon nanotubes.[20,21]

To resolve these discrepancies in the calculated entropies of single-file water, we here use the most direct method to determine the entropy of transfer, by examining the thermodynamics of filling an open carbon nanotube in equilibrium with bulk TIP3P water in molecular dynamics (MD) simulations over a range of temperatures. We first describe the simulation setup and the analysis methods, including those for periodically replicated nanotubes (with the issue of the bulk reference discussed in the Appendix). We then report free energies of water transfer from bulk into open nanotubes with slightly weakened carbon-water attractive interactions, determined directly from the logarithms of the observed water occupancy probabilities. Energies and entropies of transfer determined from the temperature dependence of these free energies are compared to the results for an infinite periodic tube obtained from the temperature dependence of the grand-canonical par-

[a)]Present address: Department of Atmospheric Sciences and Chemistry, Plymouth State University, Plymouth, New Hampshire 03264-1595, USA.
[b)]Authors to whom correspondence should be addressed. Electronic addresses: rasaiah@maine.edu and gerhard.hummer@nih.gov.

tition function, and to the results obtained by using expressions for the entropy based on model calculations of the density of states of confined water.[20,21] We find that the entropies of transfer of water into the (6,6) carbon nanotubes are negative and filling is driven by the energy of transfer both for open and periodically replicated nanotubes of subnanometer diameters. New Monte Carlo simulations of water in infinite periodic tubes show that the entropy of transfer per particle increases with increasing pore diameter in the range 0.77–0.83 nm, but this increase is not sufficient to produce a significant entropy gain. Our conclusion that filling is driven by the energy of transfer opens up the prospect of constructing a water switch in which the nanotube can be emptied or filled by changing the temperature, as well as by fine tuning the nanotube-water interaction, by chemical modification, or by the imposition of an external field.

II. METHODS

A. MD simulations of open nanotubes

We determined the thermodynamics of filling a short nanotube of length ∼1.35 nm and diameter ∼0.806 nm open to the surrounding water reservoir at both ends. The (6,6) "armchair"-type carbon nanotube was constructed by rolling up a graphene sheet of 5 × 12 carbon rings into a cylinder. This tube was then solvated with 1034 TIP3P (Ref. 22) water molecules. The nanotube-water interactions were treated as in earlier studies,[1,2] as summarized below. To probe partially filled states, we modified the attractive term of the carbon-water Lennard-Jones potential by a control parameter λ,

$$U(r,\lambda)=4\varepsilon\left[\left(\frac{\sigma}{r}\right)^{12}-\lambda\left(\frac{\sigma}{r}\right)^{6}\right]=4\varepsilon'\left[\left(\frac{\sigma'}{r}\right)^{12}-\left(\frac{\sigma'}{r}\right)^{6}\right] \tag{1}$$

resulting in a modified Lennard-Jones form with effective parameters $\varepsilon' = \varepsilon\lambda^2$ and $\sigma' = \sigma/\lambda^{1/6}$ (see Table I). Previous studies of water in short and long nanotubes showed that the filling of the nanotube is extremely sensitive to the strength of the water-carbon potential. By fine-tuning the parameter λ controlling the nanotube-water interaction, conditions can be found at which the open nanotube fluctuates between filled and empty states.[1,2] The system can also be switched to a completely filled or a completely empty state by adjusting the nanotube-water interaction potential. Similar observations were made for the SPC/E water model, with filling transitions of (6,6) nanotubes reported at ∼8.5% and ∼10% relative humidity for TIP3P (Ref. 18) and SPC/E (Ref. 23) water at ambient conditions, respectively, suggesting that our results depend weakly on the water model. To maintain continuity and permit easy comparison with previous work[1,2] we use the TIP3P water model.

TABLE I. Lennard-Jones parameters of the λ-dependent carbon-water interactions.

λ	ϵ' (kJ/mol)	σ' (nm)
1.000	0.478 357	0.32 752
0.785	0.294 763	0.34 101
0.752	0.270 537	0.34 345

The MD simulations were performed with the sander modules of the AMBER 6 and 10 program suites (University of California, San Francisco).[24] A constant pressure of 1 bar and temperatures of $T = 280$, 290, 300, 310, and 320 K were maintained with the weak-coupling barostat and thermostat (AMBER 6),[25] and the Andersen thermostat[26] and the weak coupling barostat (AMBER 10), respectively. Particle-mesh Ewald summation[27] was used for the long-range electrostatics. A time step of 2 fs and real space cut-offs of 1 nm (AMBER 6) and 1.3 nm (AMBER 10) were used. Other details are as in Ref. 2. After equilibration, the length of the periodically replicated cubic simulation box was ∼3.3 nm. The AMBER 6 production runs were carried out for 63 ns for $\lambda = 0.752$ and 0.785 at each of the five temperatures, and for 5 ns for $\lambda = 1.0$. The overall simulation time was 655 ns. The AMBER 10 production runs extended for 85 ns each at $\lambda = 0.785$, 0.8, 0.9, and 1.0, with a combined production time of 1.7 μs. Unless stated otherwise, results are for the simulations using the weak-coupling thermostat.

Water occupancy values N in the nanotubes were determined as previously,[1,2] with the nanotube interior defined as the cylindrical volume bounded at the two ends by the carbon atoms at the rims. Occupancy probabilities $P(N)$ were determined as averages of the occupancy indicator functions. Errors of time averaged observables were estimated from their time correlation functions (with the square standard error of the mean given by two times the estimated variance of the observable multiplied by its correlation time and divided by the simulation time; used for AMBER 6 runs) and from standard block averages (AMBER 10 runs), combined with linear error propagation for derived quantities, in particular slopes and intercepts of line fits, but ignoring cross correlations. To estimate the correlation time, we used the integral of bi-exponential fits to the time correlation functions.

B. Thermodynamics of water transfer

The Helmholtz free energy of transferring N water molecules from a reservoir into a nanotube is related to the occupancy probability $P(N)$ by[3]

$$\Delta A_N = -k_B T \ln\frac{P(N)}{P(0)} + NpV_{\text{bulk}}, \tag{2}$$

where k_B is Boltzmann's constant, T is the absolute temperature, p is the pressure, V_{bulk} is the volume per particle in the bulk phase, and $P(0)$ is the probability that the nanotube is empty. In the following, we neglect the small pressure-volume term of about $pV_{\text{bulk}} = 1.8 \times 10^{-3}$ kJ/mol at ambient conditions.[3] Since $\Delta A_N = \Delta U_N - T\Delta S_N$ it follows that

$$\beta\Delta A_N = -\ln\frac{P(N)}{P(0)} = \frac{\Delta U_N}{k_B T} - \frac{\Delta S_N}{k_B}, \tag{3}$$

where ΔU_N and ΔS_N are the energy and entropy differences between N water molecules in the nanotube and in bulk water, and $\beta^{-1} = k_B T$. From a straight-line fit to $\beta\Delta A_N/N = -\ln[P(N)/P(0)]/N$ as a function of T^{-1}, one ob-

tains $\Delta U_N/(k_B N)$ from the slope and $\Delta S_N/(k_B N)$ from the intercept, assuming they are both essentially constant over the temperature range of the fit. If this assumption were violated, we should see systematic deviations from linearity in the fit. Under the assumption of linearity, the same values are obtained by fitting a straight line to ΔA_N as a function of T and determining the entropy from its slope, $\Delta S_N = -\partial \Delta A_N/\partial T$, which was confirmed also numerically. The energy and entropy of transfer can thus be determined from the temperature dependence of the free energy of transfer.

We also estimated the enthalpy and entropy of transfer from the total enthalpy $U + pV$ of the entire system and the free energies calculated from $P(N)$. For this, we calculated $T\Delta S_N = \langle U + pV\rangle_N - \langle U + pV\rangle_o - \Delta A_N$, where the averages are over conformations of given occupancies N and 0, respectively. Independent entropy estimates were obtained at each of the five temperatures simulated with the Andersen[26] thermostat, and the results were then averaged.

To combine results from simulations at different values of λ and at different temperatures we adapted a thermodynamic integration method. We note that histogram methods could not be used because the weak-coupling barostat available in AMBER 6 and AMBER 10 does not produce a strict isothermal-isobaric ensemble.[25] In the thermodynamic integration, we performed a global chi-square fit of the free energy function $\Delta A_N(T, \lambda) = h_{0N} + h_{1N}\lambda + h_{2N}\lambda^2 + \cdots - T(s_{0N} + s_{1N}\lambda + s_{2N}\lambda^2 + \cdots)$ to the free energy estimates obtained from occupancy probabilities $P(N; T,\lambda)$ and to the estimated derivatives $\partial \Delta A_N/\partial\lambda = -4\varepsilon\sigma^6\langle\sum r_{ij}^{-6}\rangle_N$, where the sum extends over all carbon-oxygen pairs within the cutoff range and the average is over states with fixed N. As fit models, we tested polynomials of different order in λ for the entropy and enthalpy.

C. Infinite periodic nanotubes

Vaitheeswaran *et al.*[3] reported on Monte Carlo simulation studies of the temperature dependence of water confined to a 1D periodically replicated nanotube. Without direct interactions with an external water reservoir, the filling equilibrium was determined by constructing the grand-canonical partition function of water confined into the nanotube term by term. To maintain the periodicity of the carbon lattice in the (6,6) nanotube with 0.806 nm diameter, the length of the 1D periodic cell was fixed at $L = 1.453$ nm which is slightly longer than our open tube of length 1.36 nm. As noted earlier,[3] the filled states correspond to five and six water molecules in the open and periodic unmodified tubes, respectively.

To study the effects of the average particle spacing, $\Delta z = L/N$, tube length, and tube diameter on the thermodynamics of filling, we performed additional Monte Carlo simulations of infinite periodic tubes. We used different repeat lengths L of 1.453, 2.664, and 3.875 nm, and different pore diameters $D = 0.777$ and 0.835 nm, in addition to the original diameter of 0.806 nm. These wider and narrower pores were obtained by uniformly scaling the carbon-carbon bond lengths, which resulted in corresponding changes in the repeat lengths L.

For these periodic tubes, the free energy of transfer of water was determined by constructing a grand-canonical ensemble using successive ratios of probabilities

$$\frac{P(N+1)}{P(N)} = \frac{\rho V e^{\beta\mu^{ex}_{\text{bulk}}}}{N+1}\langle e^{-\beta(U_{N+1}-U_N)}\rangle_N, \tag{4}$$

where μ^{ex}_{bulk} is the excess chemical potential of the bulk fluid at a density ρ and temperature T , and $\langle e^{-\beta(U_{N+1}-U_N)}\rangle_N = \langle e^{-\beta(U_N-U_{N+1})}\rangle^{-1}_{N+1} \equiv e^{-\beta\mu^{ex}_N}$ defines the excess chemical potential of N water molecules in the nanotube and is equal to the Boltzmann averages of the binding energy of an $(N + 1)$-th molecule randomly inserted into a volume V that covers the nanotube and already contains N water molecules, and of a particle removed from an $(N + 1)$-particle system.[17] Here, we used the Bennett acceptance ratio method[28] to calculate μ^{ex}_N from the energy distributions for particle insertion and removal. In the simulations, the ratio $P(N)/P(0)$ for $N \geq 1$ is determined by recursive application of Eq. (4) and subsequent normalization.

Unlike the simulations of the open nanotubes conducted here, for infinite periodic tubes the bulk reference state has to be defined explicitly. In particular, the ratio $P(N + 1)/P(N)$ in Eq. (4) depends on both the excess chemical potential μ^{ex}_{bulk} and the density ρ of the bulk fluid. Here we obtained these properties from simulations of bulk TIP3P water, as described below in the Appendix and presented in Table III.

III. RESULTS AND DISCUSSION

The MD simulations were initiated from a structure with an empty nanotube immersed in a water reservoir. With the water-nanotube interaction parameter $\lambda = 1$ corresponding to the unmodified Lennard-Jones interaction between the water and the nanotube, the nanotube was found to fill up rapidly and then to remain filled. Figure 1(a) shows a slab view of the nanotube filled with water and surrounded by a water reservoir. Figure 1(b) shows a close-up view of the single-file chain of H-bonded water molecules in the nanotube.

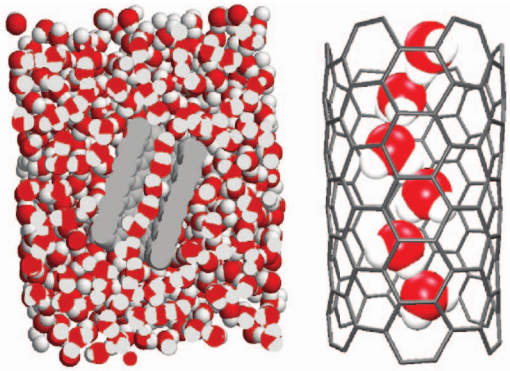

(a) (b)

FIG. 1. Simulation system. (a) Slab view of the nanotube filled with water and surrounded by water reservoir. (b) Close-up of the single file of H-bonded water molecules inside the nanotube.

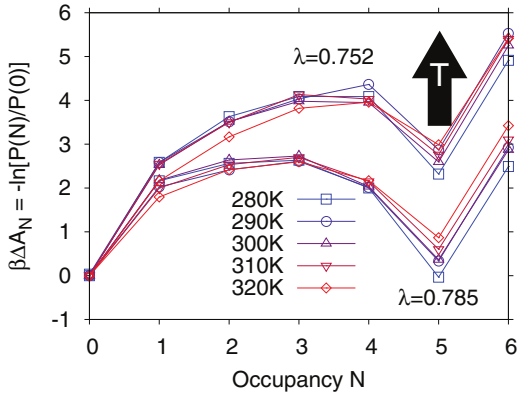

FIG. 2. Free energies of transfer of water into a (6,6) nanotube open to a reservoir as a function of the occupancy number N for temperatures ranging from 280 K to 320 K for $\lambda = 0.752$ and 0.785.

A. Dependence of water occupancy on nanotube-water interactions and temperature

Figure 2 shows the free energy of transfer in units of k_BT, $\beta\Delta A_N = -\ln[P(N)/P(0)]$, as a function of the number of water molecules N transferred into the open nanotube from the surrounding water bath at temperatures from 280 to 320 K for $\lambda = 0.752$ and $\lambda = 0.785$. The two minima at $N = 0$ and 5 corresponding to the empty and completely filled states are separated by a barrier at intermediate filling states. As λ increases from 0.752 to 0.785, the free energy barrier decreases and filling becomes more favorable. Changing the parameter λ controlling the strength of the attractive $1/r^6$ carbon-water interactions thus had the effect expected from earlier simulations[1,2] on the water filling equilibrium. For $\lambda = 1$ at 300 K, the tube remained filled for the duration of the simulations, which eliminates the possibility of determining the probability $P(0)$ of the empty state directly; for $\lambda = 0.785$, the tube fluctuated between an empty and filled state, both having roughly the same population; and for $\lambda = 0.752$, the tube was predominantly empty, with rare fluctuations to a completely filled state (see Figs. 3 and 8 of Ref. 2). The results obtained from the simulations with the Andersen[26] thermostat agree quantitatively with the weak-coupling[25] thermostat data for $\lambda = 0.785$. For $\lambda = 0.8$, the filled state was predominant; for $\lambda = 0.9$, we observed transient emptying only at 300 K and above, and again no emptying at $\lambda = 1$. Evidently, the free energy of transfer of water from an external reservoir into the nanotube decreases and filling becomes more favorable as the attractive interaction with the nanotube increases from $\lambda = 0.752$ to 1.0 at 300 K.

An increase in temperature shifts the filling equilibrium toward the empty state. Figure 3 shows the water occupancy as a function of time at 280, 300, and 320 K for $\lambda = 0.785$. During the 63 ns simulations, a significant number of transitions occurred between the empty and filled states at all temperatures, allowing us to determine accurate occupancy probabilities $P(N)$, which are also shown in Fig. 2. We find that the probabilities of filled and empty states are equal at 280 K, but this balance is tipped towards the empty state as the temperature rises to 320 K. A similar shift towards emptying at higher temperatures was obtained for $\lambda = 0.752$. These results

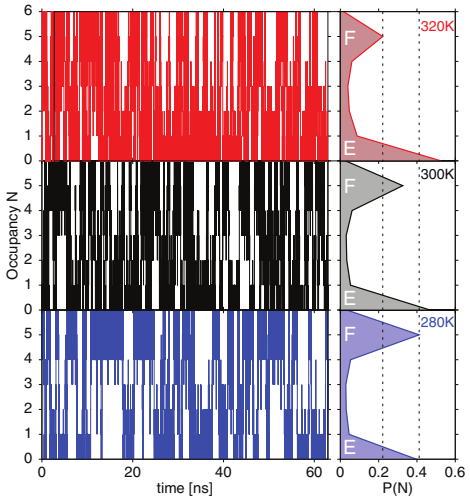

FIG. 3. Sensitivity of water occupancy in the open (6,6) nanotubes to temperature. The left panels show the water occupancy N as a function of time from MD simulations at $T = 280$, 300, and 320 K (bottom to top) with nanotube-water attractive interactions scaled by $\lambda = 0.785$. The right panels show the corresponding normalized occupancy histograms $P(N)$. Dashed vertical lines indicate the probability $P(N = 5)$ of the filled state at the lowest and highest temperature simulated.

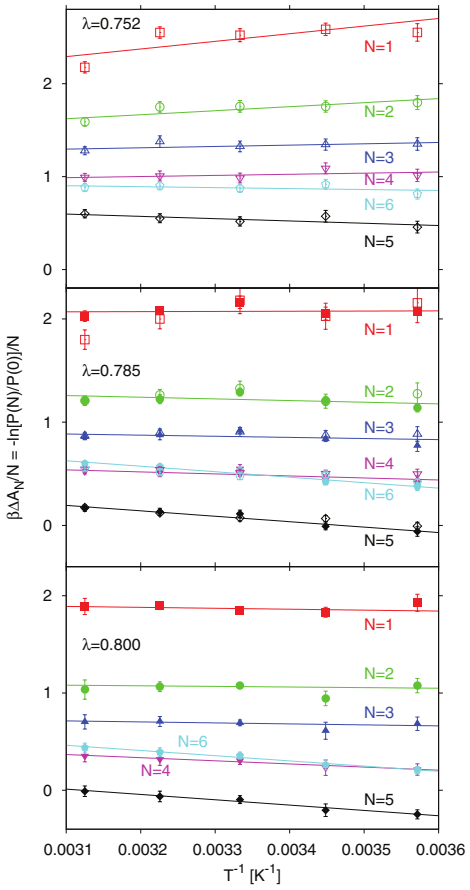

FIG. 4. Transfer free energy per water molecule in units of k_BT as a function of the inverse temperature for open (6,6) nanotubes immersed in TIP3P water. The energy of transfer ($\Delta U_N/N$) and entropy of transfer ($-\Delta S_N/Nk_B$) are obtained from the slope and intercept, respectively, of lines fitted to the MD data obtained with the Andersen thermostat (middle, bottom) and weak-coupling thermostat (top). Results are shown for $\lambda = 0.752$ (top), $\lambda = 0.785$ (middle), and $\lambda = 0.8$ (bottom) between 280 and 320 K (filled symbols: Andersen[26] thermostat; open symbols: weak-coupling[25] thermostat).

TABLE II. Thermodynamics of transferring TIP3P water into an open and solvated nanotube at $T = 300$ K in units of kJ/mol for $\lambda = 0.752$ and 0.785. Results for the completely filled $N = 5$ state are in italics. The first and second line for each N list the results obtained from fits of the temperature dependence; the third line lists the results obtained directly from differences of the system enthalpies and free energies. Results in line one for each N are for weak-coupling thermostat simulations,[25] and in lines two and three for Andersen[26] thermostat simulations. Numbers in parentheses indicate estimated statistical errors in the last digits.

	$\lambda = 0.752$			$\lambda = 0.785$		
N	ΔU_N	$T\Delta S_N$	ΔA_N	ΔU_N	$T\Delta S_N$	ΔA_N
1	6.8(1.7)	0.6(1.7)	6.2	6.3(3.1)	1.3(3.0)	5.0
				0.1(0.9)	−5.0(0.9)	4.9
				1.9(3.0)	−3.6(3.0)	5.5
2	7.2(2.8)	−1.4(2.8)	8.6	1.7(3.2)	−4.6(3.1)	6.3
				−2.7(2.0)	−8.8(2.0)	6.1
				−2.0(3.0)	−8.2(3.0)	6.2
3	3.6(3.9)	−6.4(3.9)	10.0	0.7(3.4)	−6.0(3.4)	6.7
				−2.7(2.5)	−9.1(2.5)	6.4
				−6.8(2.4)	−13.0(2.4)	6.2
4	4.0(5.1)	−6.1(5.1)	10.1	−4.0(3.3)	−9.2(3.2)	5.2
				−6.5(3.8)	−11.4(3.7)	4.9
				−7.6(2.0)	−12.5(2.1)	4.9
5	*−10.3(6.4)*	*−17.0(6.3)*	*6.7*	*−15.3(3.5)*	*−16.4(3.5)*	*1.1*
				−21.9(4.3)	*−22.7(4.2)*	*0.8*
				−17.2(2.0)	*−18.0(1.9)*	*0.8*
6	−5.1(7.0)	−18.3(6.9)	13.2	−12.9(3.9)	−20.3(3.8)	7.4
				−26.5(4.2)	−34.0(4.1)	7.5
				−22.7(2.1)	−30.2(2.0)	7.5

suggest that the free energy of filling the pore becomes less favorable (more positive) with rising temperature, and that the corresponding entropy of transfer is negative.

B. Entropy of transfer

The most direct and unambiguous method of obtaining the energy and entropy of transfer of water from a reservoir into a nanotube as a function of the occupancy N is from the temperature dependence of the free energy of transfer. In Fig. 4, $\beta\Delta A_N/N = -\ln[P(N)/P(0)]/N$ is plotted against the inverse temperature $1/T$ for the open nanotube at $\lambda = 0.752$, 0.785, and $\lambda = 0.8$ for which the free energies of transfer into the open nanotube could be determined directly (see Sec. III A). According to Eq. (3), the slope and intercept of straight-line fits to the data in Fig. 4 give the transfer energies and entropies per water molecule, respectively.

We find from this thermodynamic analysis that the entropy of transfer $\Delta S_{N=5}$ of the completely filled state is negative for the open tube. Table II lists the entire set of energies ΔU_N, entropies ΔS_N, and free energies of filling an open nanotube with N water molecules at 300 K for $\lambda = 0.752$ and 0.785. Even for the transfer of the first water molecule into the open tube, our calculations show no significant gain in entropy, which reflects the strong coupling of this water molecule to the surrounding bulk fluid through hydrogen bond and electrostatic interactions. For subsequent entries into the open tube, the entropy of transfer becomes negative, i.e., unfavorable.

Estimates of the enthalpy and entropy of transfer from differences in the total system enthalpies and the free energies calculated from $P(N)$ are consistent with the results obtained by fitting the temperature dependence (see Table II). The results are also independent of the thermostat used in the simulations (with the possible exception of the poorly sampled $N = 6$ state). In particular, for both thermostats we find that the $N = 5$ filled state has a lower entropy than the empty state.

This negative entropy of transfer for the completely filled ($N = 5$) state of an open nanotube agrees qualitatively with the entropy of transfer for an infinite periodic tube, a system without possible end effects, as in a short tube. In Fig. 5, we show that the entropy of transfer into an infinite periodic tube with $\lambda = 1$ depends linearly on the spacing per particle $\Delta z = L/N$ over the range between 0.2 and 0.3 nm bracketing the completely filled state. The entropies obtained in the earlier study for $L = 1.453$ nm,[3] after correction for the equation of state of TIP3P water as described in the Appendix, are consistent with the new results. For the spacing $\Delta z = 0.26$ nm seen in the open nanotube,[1] the entropy of transfer into the periodic tube is about $-0.5\ k_B$ per particle. The corresponding value for the open tube with $N = 5$ water molecules is about $-1.3\ k_B$ (Table II). Importantly, both entropies are negative. The somewhat larger loss of entropy in the open tube could be the result of end effects.

To quantify the dependence of the entropy of transfer on the pore diameter, we performed Monte Carlo simulations of water in infinite periodic tubes of different diameters, which we obtained by scaling the carbon-carbon bond length. We found the transfer entropy per particle to increase with increasing pore diameter (Fig. 5; top). For $\Delta z = 0.26$ nm and diameters of 0.777, 0.806, and 0.833 nm, the entropy per particle increased from about -1 to -0.5 and 0 k_B, respectively.

We noted previously[3] that for the infinite periodic tube, the transfer entropies are independent of carbon-water

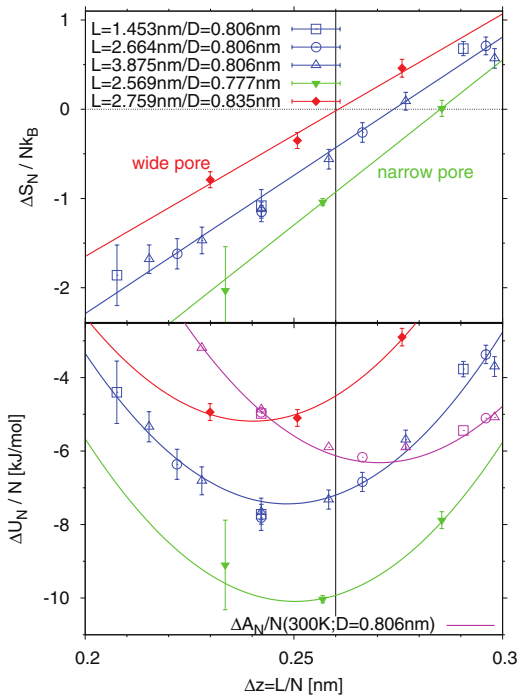

FIG. 5. Entropy (top) and energy (bottom) of transfer per water molecule in infinite periodic tubes with $\lambda = 1$ and different repeat lengths L and diameters D as a function of the average spacing per particle $\Delta z = L/N$ along the tube axis at 300 K. Wide and narrow pores of diameters 0.835 nm and 0.777 nm were obtained by scaling the carbon-carbon bond lengths of the original pore ($D = 0.806$ nm) from 0.14 nm to 0.145 and 0.135 nm, respectively. The vertical line indicates the equilibrium spacing of $\Delta z \approx 0.26$ nm in the open nanotube.[1] Lines are linear and quadratic fits to the entropy and energy, respectively. The bottom plot shows $\Delta U_N/N$ (symbols with error bars: from Monte Carlo simulations), and $\Delta A_N/N$ (magenta line: obtained by combining the fits to the energy and entropy; symbols: from Eqs. (2) and (4)) for the original pore diameter ($D = 0.806$ nm).

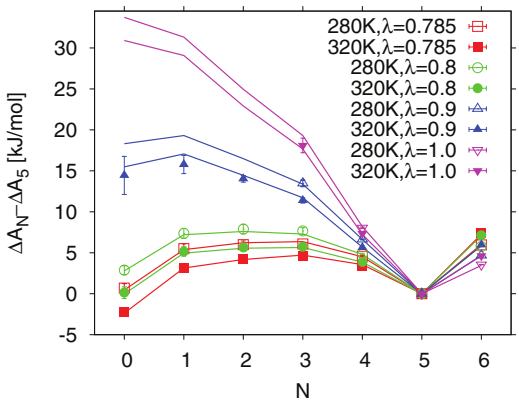

FIG. 6. Comparison of transfer free energies $\Delta A_N - \Delta A_5$ for different values of λ calculated directly from the logarithm of the occupancy probabilities (open symbols: 280 K; filled symbols: 320 K), and from global fits to the free energies and free energy derivatives with respect to λ (upper and lower lines for $N<5$ are at 280 and 320 K, respectively). In the fits, the entropy and enthalpy were assumed to be constant and quadratic polynomials in λ, respectively.

attraction strength, $\lambda = 0.752$, 0.785, and 1.0. Here, we found that for open nanotubes with $\lambda = 0.752$ and 0.785 the entropies again agree within statistical errors (Table II). We also combined results from simulations at different values of λ and at different temperatures by thermodynamic integration (see Sec. II B). We found that for given N, we could fit the data well with a second order polynomial in λ for the enthalpy and a constant entropy (with all data fitted within their expected statistical error on average; see Fig. 6). Making the entropy depend linearly or quadratically on λ did not significantly improve the fit. From the global fits we estimate $T\Delta S_{N=5} = -22$ kJ/mol at 300 K, in agreement with the other estimates in Table II. We conclude from this consistency and independence of λ that the entropy is determined primarily by geometric effects (such as the pore diameter) and intrinsic properties of the hydrogen-bonded water chains (i.e., residual rotational and translational freedom), and less by extrinsic properties such as the carbon-water attractive interaction strength.

C. Energy of transfer

The results in Table II show that for $\lambda = 0.752$ and 0.785 the energies of transfer are positive for partially occupied tubes, but negative and thus favorable for the completely filled states. As expected, the transfer energy decreases with increasing carbon-water attraction strength λ. First-order perturbation theory accounts for the constant difference of 1.45 $\pm$ 0.69 kJ/mol per water molecule for $N = 1$–5 between the transfer energies for $\lambda = 0.752$ and 0.785. On the basis of the linear λ dependence of the energy of transfer obtained previously for infinite periodic tubes in vacuum,[3] we expect a difference of 7.5 kJ/mol (0.785–0.752)/(1–0.752) = 1 kJ/mol, in excellent agreement with our results obtained here for open tubes in aqueous solution. Over the entire range up to $\lambda = 1$, we found that we needed to include a small quadratic λ^2 correction (Fig. 6).

For partially filled tubes ($N < 5$), transfer into the open tube is more favorable than into the periodic tube (Table II and Ref. 3). This difference in energies reflects the favorable interactions even of fragmented water chains in the open tube with the surrounding bulk fluid. We also note that in the open tube, the transfer energy per molecule is almost independent of N for $1 < N < 5$. We showed previously[2] that newly entering water molecules are preferentially attached to the growing chain of single-file water. Ignoring long-range interactions and polarization effects, such a process indeed explains the weak N dependence of the transfer energy per molecule. We note that in open tubes for $N = 6$ the transfer energy per molecule is higher than for $N = 5$. The likely explanation for this increase is that the $N = 6$ chain is compressed. Indeed, for the infinite periodic tubes we found that the energies of transfer depend approximately quadratically on the particle spacing Δz close to the filled state (Fig. 5 bottom).

So what is the thermodynamic driving force for filling? Figure 7 shows the transfer free energy, energy, and entropy for the open, solvated tubes as a function of the water occupancy for two values of the carbon-water interaction strength. We found that there is entropy-energy compensation, with a strong energetic driving force for filling overcoming an unfavorable entropy.

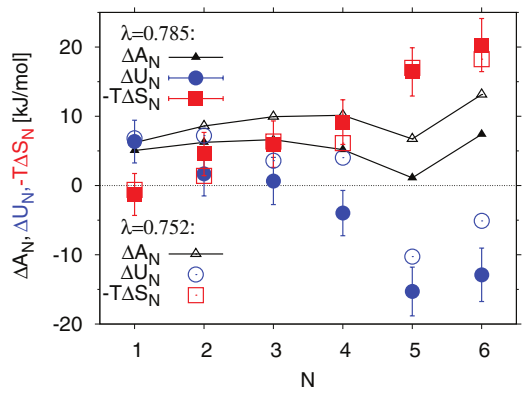

FIG. 7. Thermodynamic driving force and entropy-enthalpy compensation for water filling of the (6,6) nanotube at 300 K. Free energy (black triangles), energy (blue circles), and entropy of transfer (red squares) as a function of the occupancy for $\lambda = 0.752$ (open symbols) and 0.785 (filled symbols).

IV. CONCLUSIONS

We used MD simulations to determine the entropy and energy of single-file water confined into narrow carbon nanotubes. For pores filled with continuous single files of hydrogen bonded TIP3P water molecules open to a reservoir, we found that the entropy of transfer is negative. The entropy of water in such narrow nanopores is thus lower than in the bulk phase. As a consequence, increasing temperature results in an increased free energy of transfer, and eventual emptying of the pore.

Our result of a negative entropy of transfer appears to be in contradiction with results published by two of us before.[3] Vaitheeswaran *et al.*[3] previously studied a periodically replicated isolated carbon nanotube and reported small but positive transfer entropies for $N = 5$ but negative entropies of transfer for $N = 6$. Here we showed that this apparent difference disappears if we use the equation of state of bulk TIP3P water instead of real water as a reference and account for the dependence of the transfer entropy on the water spacing Δz. Consequently, we found negative entropies of transfer also for infinite periodic tubes when using the bulk TIP3P equation of state. The entropy of transfer of bulk TIP3P water into nanotubes is thus negative for the filled state in both open tubes solvated in water and in infinite periodic tubes in vacuum. These consistent results were obtained with different simulation methods (MD and Monte Carlo) and analyzed in different ways [by determining $P(N)$ from counting and by constructing $P(N)$ recursively from the grand-canonical partition function, respectively].

The negative entropy of transfer found here also appears to contradict results obtained recently by Kumar *et al.*[21] and by Pascal *et al.*[20] who studied TIP3P water in (6,6) carbon nanotubes and reported positive transfer entropies of $\sim 0.9\ k_B$ and $\sim 5\ k_B$ per molecule, respectively. These results were obtained from molecular simulations analyzed with an approximate density of states model for the entropy. These positive transfer entropies contrast with our negative entropies of $-1.3\ k_B$ and $-0.5\ k_B$ for water in open and infinite periodic tubes, respectively. Since Pascal *et al.*[20] found essentially unchanged results for TIP3P and SPCE water, we can rule out force field differences as a main cause of this discrepancy. However, there are small differences in the pore diameter (0.835 in Ref. 20 vs. 0.806 nm here) and the spacing of water molecules Δz ($\sim$0.28 vs. 0.26 nm here). On the basis of our data for the infinite periodic tube in Fig. 5(a), the entropy of transfer into this wider and less tightly filled tube would indeed be higher, about $0.5\ k_B$. Whereas this corrected entropy is positive and close to the value reported by Kumar *et al.*,[21] it is still much lower than the value of $5.4\ k_B$ reported by Pascal *et al.*[20]

Since our analysis is essentially without any assumptions – we simply monitor the relative population of the filled state as a function of temperature – it would seem that the likeliest cause of the discrepancies is the use of an approximate formalism to calculate entropies in the other studies. However, while we checked that our MD results are independent of the choice of weak-coupling[25] and Andersen[26] thermostat, and of the real-space cutoff distance, it is conceivable that other simulation parameters, such as the length of the open tube, could be relevant factors; but considering the magnitude of the effect and the agreement with Monte Carlo simulations in the canonical ensemble conducted with a different program,[3] such alternative explanations seem unlikely to resolve the issue.

Our results for open tubes also confirm our earlier finding for infinite periodic tubes[3] that the entropy of water in fully formed single-file chains is largely insensitive to the carbon-water interaction strength. In contrast, the energy of transfer is highly sensitive to the carbon-water interaction strength, which in turn affects the free energy of transfer.[1,2] However, as was already shown by Vaitheeswaran *et al.*,[3] this dependence of the energy on the carbon-water interaction strength can be accounted for almost fully by a mean-field type correction that appropriately scales the average water-pore attractive interaction energy.

The energy of transfer emerges as a major factor in the transfer process. This energetic dominance appears to contradict the notion that carbon nanotubes are hydrophobic and should repel water. But, as shown here, the transfer energy into a subnanometer nanotube is determined by the loss of interactions in the bulk phase, traded off by gains through tight hydrogen bonds in the single-file chains, and significant dispersion interactions with the pore. In "real" carbon nanotubes, we expect in addition strong polarization effects not accounted for in the present study, in particular for water in metallic tubes. We note further that the entropy of transfer increases with diameter of the tube and can become positive for larger diameters.

We conclude from our results that narrow nanotubes filled by single-file water should "dry" at elevated temperatures, resulting in behavior reminiscent of liquid-gas phase transitions on heating.[18,29] Recent experiments by Wu and coworkers[30] indeed showed drying, albeit for tubes of slightly larger diameter (1.4 nm) in which water is not expected to form single-file chains. So the question whether single-file water has larger or smaller entropy than bulk water remains open, both with respect to the differences between different computational results, and with respect to a decisive experimental test.

ACKNOWLEDGMENTS

The authors thank Dr. S. Vaitheeswaran and Dr. H. Yin for discussions. J.C.R. thanks the National Science Foundation for support under Grant No. CHE 05489187. A.W. and J.C.R. thank the University of Maine Supercomputing Cluster for generous allocations of computing time and resources and Dr. John Koskie and Dr. Steve Cousins for their assistance. G.H. is supported by the Intramural Research Program of the National Institute of Diabetes and Digestive and Kidney Diseases, National Institutes of Health. This study utilized the high-performance computational capabilities of the Biowulf PC/Linux cluster at the National Institutes of Health, Bethesda, MD (http://biowulf.nih.gov).

APPENDIX: EQUATION OF STATE OF TIP3P WATER

We determined the equation of state of TIP3P water near ambient conditions from simulations at temperatures $T = 280$, 290, 300, 310, and 320 K. These simulations were carried out with the sander module of AMBER 9 (University of California, San Francisco). We simulated a system of $N = 1024$ rigid TIP3P water molecules using a time step of 2 fs, particle-mesh Ewald summation[27] with a mesh width of ~0.1 nm and cubic-spline interpolation, and a real-space interaction cutoff of 1.3 nm. Production runs extended for 6 ns, with structures saved every 0.5 ps. The box sizes of the constant-volume runs were chosen to produce pressures close to 1 bar based on a preliminary estimate of the equation of state. Small deviations from the target pressure were corrected perturbatively, as described in the following paragraph. For comparison, we also performed 10-ns long simulations at each of the temperatures with a shorter cutoff of 1 nm, which produced consistent results. In all simulations we used an Andersen thermostat.[26] In earlier simulations using a Langevin integrator we noticed small but significant deviations from the target temperature, with actual kinetic temperatures being too high by ~0.06 K.

To determine the bulk excess chemical potential we performed particle removal and test-particle insertion calculations. Ewald summation was used for the electrostatic interactions. The resulting energy distributions were analyzed by using Bennett's acceptance ratio method.[28] We also used Bennett's overlapping histogram method[28] to check for consistency of the energy distributions. To correct for small deviations of the actual pressure p in our constant-volume simulations from the target pressure $p_0 = 1$ bar, we used $\mu^{ex}_{\rm bulk}(p_0) \approx \mu^{ex}_{\rm bulk}(p) + (p_0 - p)/\rho$, which follows from the Maxwell relation $(\partial \mu^{ex}_{\rm bulk}/\partial p)_{T,N} = \rho^{-1}$. Pressure corrections of the density in Eq. (4) are expected to be small and were thus neglected, based on an isothermal compressibility of $\sim 5.7 \times 10^{-5}$ bar^{-1} of TIP3P water at 300 K, as obtained from simulations at different densities.

Errors in the bulk excess chemical potentials were estimated from block averages. For pressures and internal energies, we determined the correlation times τ by integration of a bi-exponential fit to the normalized autocorrelation function. Statistical errors σ in the mean were then estimated by scaling the variance v of the respective observable, $\sigma^2 = 2\tau v/t$, where t is the total simulation time. According to $s^{ex}_{\rm bulk} = -(\partial \mu^{ex}_{\rm bulk}/\partial T)_{p,N}$, we extracted an excess entropy per particle of $s^{ex}_{\rm bulk} = -5.88 \pm 0.12\ k_B$ at 300 K from linear fits to the excess chemical potential as a function of temperature at a constant pressure of 1 bar. We confirmed that this result agrees with the temperature-dependent entropy obtained via $s^{ex}_{\rm bulk} = (U + pV)/NT - \mu^{ex}_{\rm bulk}/T$, as listed in Table III together with the other results of the bulk TIP3P simulations ($s^{ex}_{\rm bulk} = -5.81 \pm 0.01\ k_B$ at 300 K).

To connect to experiment, Vaitheeswaran *et al.*[3] used the chemical potential of TIP3P water in their simulations (−25.3 kJ/mol at 298 K), but the temperature dependence, measured chemical potential, and density of water as reference (Table II of Ref. 3). To connect to the simulations of the open nanotubes in TIP3P water performed here, a reference state correction has to be applied to the thermodynamic data of filling reported in Ref. 3, as already discussed there. From Eq. (4), we have

$$\left[\frac{P(N)}{P(0)}\right]_{\rm TIP3P} = \left[\frac{P(N)}{P(0)}\right]_{\rm wat} R^N;$$
$$\text{with } R = \frac{\rho^{\rm TIP3P}_{\rm bulk}}{\rho^{\rm wat}_{\rm bulk}} e^{\beta(\mu^{ex,{\rm TIP3P}}_{\rm bulk} - \mu^{ex,{\rm wat}}_{\rm bulk})}, \tag{A1}$$

where "TIP3P"and "wat" refer to the equations of state of TIP3P and real water, respectively. The resulting correction to the free energy is

$$\begin{aligned}\Delta A_N({\rm TIP3P}) - \Delta A_N({\rm wat}) &= -k_B T \ln \frac{[P(N)/P(0)]_{\rm TIP3P}}{[P(N)/P(0)]_{\rm wat}} = -N k_B T \ln R \\ &= -N k_B T \ln\left(\rho^{\rm TIP3P}/\rho^{\rm wat}\right) - N\left(\mu^{ex,{\rm TIP3P}}_{\rm bulk} - \mu^{ex,{\rm wat}}_{\rm bulk}\right).\end{aligned} \tag{A2}$$

From linear fits to the density and excess chemical potential of TIP3P water as a function of temperature (Table III), from cubic fits to the experimentally determined densities of

TABLE III. Thermodynamic properties of bulk TIP3P water and real water near ambient conditions from MD simulations in an *NVT* ensemble. The excess entropies (last column) are per particle. Numbers in parentheses indicate estimated statistical errors in the last digits.

T [K]	ρ [nm^{-3}] TIP3P	ρ [nm^{-3}] water	p [bar]	U/N [kJ/mol]	$\mu^{ex}_{\rm bulk}$ [kJ/mol]	$\mu^{ex}_{\rm bulk}$(1bar) [kJ/mol]	$s^{ex}_{\rm bulk}$ [k_B]
280	33.4614	33.4240	−0.2(6.4)	−41.053(5)	−26.38(5)	−26.38(5)	−6.30(2)
290	33.1648	33.3869	−15.2(6.4)	−40.494(4)	−25.96(3)	−25.93(3)	−6.04(1)
300	32.8717	33.3123	−4.0(6.0)	−39.950(4)	−25.46(3)	−25.45(3)	−5.81(1)
310	32.5821	33.2058	−15.4(5.7)	−39.397(4)	−24.97(2)	−24.94(3)	−5.61(1)
320	32.2958	33.0735	5.2(5.6)	−38.867(4)	−24.44(3)	−24.45(3)	−5.42(1)

water in the range 275–325 K,[31] and from the shifted chemical potential of TIP3P water used previously (Eq. (26) in Ref. 3) we obtained the free energy correction at 298 K, $\Delta A_N(\text{TIP3P}) - \Delta A_N(\text{wat}) = 0.26$ *N*kJ/mol. From the temperature derivative, we obtained $\Delta S_N(\text{TIP3P}) - \Delta S_N(\text{wat}) = -0.49Nk_B$ and $\Delta U_N(\text{TIP3P}) - \Delta U_N(\text{wat}) = -0.95$ *N*kJ/mol.

[1] G. Hummer, J. C. Rasaiah, and J. P. Noworyta, Nature (London) **414**, 188 (2001).
[2] A. Waghe, J. C. Rasaiah, and G. Hummer, J. Chem. Phys. **117**, 10789 (2002).
[3] S. Vaitheeswaran, J. C. Rasaiah, and G. Hummer, J. Chem. Phys. **121**, 7955 (2004).
[4] J. Dzubiella, R. J. Allen, and J.-P. Hansen, J. Chem. Phys. **120**, 5001 (2004).
[5] R. Allen, S. Melchionna, and J.-P. Hansen, Phys. Rev. Lett. **89**, 175502 (2002).
[6] J. Li, X. Gong, H. Lu, D. Li, H. Fang, and R. Zhou, Proc. Natl. Acad. Sci. U.S.A. **104**, 3687 (2007).
[7] L. Wang, J. Zhao, F. Li, H. Fang, and J. P. Lu, J. Phys. Chem. C **113**, 5368 (2009).
[8] K. Koga, G. T. Gao, H. Tanaka, and X. C. Zeng, Nature (London) **412**, 802 (2001).
[9] M. C. Gordillo and J. Marti, Chem. Phys. Lett. **329**, 341 (2000).
[10] Y. Maniwa, H. Kataura, M. Abe, S. Suzuki, Y. Achiba, H. Kira, and K. Matsuda, J. Phys. Soc. Jpn. **71**, 2863 (2002).
[11] H. Kyakuno, K. Matsuda, H. Yahiro, T. Fukuoka, Y. Miyata, K. Yanagi, Y. Maniwa, H. Kataura, T. Saito, M. Yumura, and S. Iijima, J. Phys. Soc. Jpn. **79**, 083802 (2010).
[12] O. Byl, J.-C. Liu, Y. Wang, W.-L. Yim, J. K. Johnson, and J. T. Yates, J. Am. Chem. Soc. **128**, 12090 (2006).
[13] M. Majumder, N. Chopra, R. Andrews, and B. J. Hinds, Nature (London) **438**, 44 (2005).
[14] J. K. Holt, H. G. Park, Y. M. Wang, M. Stadermann, A. B. Artyukhin, C. P. Grigoropoulos, A. Noy, and O. Bakajin, Science **312**, 1034 (2006).
[15] A. I. Kolesnikov, J.-M. Zanotti, C.-K. Loong, P. Thiyagarajan, A. P. Moravsky, R. O. Loutfy, and C. J. Burnham, Phys. Rev. Lett. **93**, 035503 (2004).
[16] L. Maibaum and D. Chandler, J. Phys. Chem. B **107**, 1189 (2003).
[17] J. C. Rasaiah, S. Garde, and G. Hummer, Annu. Rev. Phys. Chem. **59**, 713 (2008).
[18] J. Köfinger, G. Hummer, and C. Dellago, Phys. Chem. Chem. Phys. **13**, 15403 (2011).
[19] H. Yin, G. Hummer, and J. C. Rasaiah, J. Am. Chem. Soc. **129**, 7369 (2007).
[20] T. A. Pascal, W. A. Goddard, and Y. Jung, Proc. Natl. Acad. Sci. U.S.A. **108**, 11794 (2011).
[21] H. Kumar, B. Mukherjee, S.-T. Lin, C. Dasgupta, A. K. Sood, and P. K. Maiti, J. Chem. Phys. **134**, 124105 (2011).
[22] W. L. Jorgensen, J. Chandrasekhar, J. D. Madura, R. W. Impey, and M. L. Klein, J. Chem. Phys. **79**, 926 (1983).
[23] A. Striolo, A. A. Chialvo, K. E. Gubbins, and P. T. Cummings, J. Chem. Phys. **122**, 234712 (2005).
[24] W. D. Cornell, P. Cieplak, C. I. Bayly, I. R. Gould, K. M. Merz, D. M. Ferguson, D. C. Spellmeyer, T. Fox, J. W. Caldwell, and P. M. Kollman, J. Am. Chem. Soc. **117**, 5179 (1995).
[25] H. J. C. Berendsen, J. P. M. Postma, W. F. van Gunsteren, A. DiNola, and J. R. Haak, J. Chem. Phys. **81**, 3684 (1984).
[26] H. C. Andersen, J. Chem. Phys. **72**, 2384 (1980).
[27] T. Darden, D. York, and L. Pedersen, J. Chem. Phys. **98**, 10089 (1993).
[28] C. H. Bennett, J. Comput. Phys. **22**, 245 (1976).
[29] V. V. Chaban and O. V. Prezhdo, ACS Nano **5**, 5647 (2011).
[30] H.-J. Wang, X.-K. Xi, A. Kleinhammes, and Y. Wu, Science **322**, 80 (2008).
[31] G. S. Kell, J. Chem. Eng. Data **12**, 66 (1967).